First results from a low momentum e^+/e^- test beam at U-70 IHEP, Protvino.

G.Britvich, I.Britvich, S.Golovkin, V.Kurshetsov,
L.Landsberg, V.Maisheev, V.Molchanov, V.Semenov,
E.Vlasov, V.Zarucheisky
Institute for High Energy Physics, Protvino, Russia

February 15, 2002

1 Introduction

The main goal of the activity of the IHEP group at the channel 18T of the IHEP U-70 accelerator is to study the possibility to obtain positron beam with the low offline admixture of the other particles and relatively low energy (0.7-5 GeV). The beam is needed to study the inefficiency of the different types of guard systems for the experiments aimed to investigate the rare kaon decays (OKA-IHEP, KMN-IHEP, CKM-FNAL/IHEP, KOPIO-BNL/IHEP, etc).

Each experiment has its own requirements for the inefficiency of the guard system in this range of energy. For example, CKM experiment to study the very rare decay $K^+ \to \pi^+\nu\bar{\nu}$ requires the inefficiency to be less than $3{\cdot}10^{-5}$.

2 The Channel

In its current configuration the magnetic optics of the CH18 consists basically of three dipole magnets (M), two pairs of quadrupole magnets (Q) and a set of collimators. Two internal targets (35/1 and 35/2) can be used to produce secondary beam from the main proton beam of the U-70 accelerator. The last dipole magnet (M_7) can be rotated in the horizontal plane thus allowing to direct positron beam to the test zone. We can imagine different ways to obtain the electron beam. Some of them are presented in Fig. 1.

In the first scheme the vacuum chamber of block 35 serves as a converter for photons from the decays of secondary π^0s produced on the 35/1 target. The effective point of the conversion is determined by the current in the first dipole magnet M_1.

In the second scheme the target 35/2 of block 35 serves as a source of photons from the decays of secondary π^0s produced on it. The conversion of the photons produced at the angle of 220 mrad relative to the primary beam takes place on a special converter installed after M_1-magnet. The current in M_1 is set to be at its maximum and it serves as a sweeping magnet.

These two schemes were tested during December 2001 RUN.

The third scheme requires the modification of the vacuum chamber and target stand of block 35 and can be possibly tested in the future.

3 Beam test configuration

A view of the setup used in the December 2001 RUN is shown in Fig. 2 and in a more schematic way in Fig. 3. It consists of the stationary detectors of the channel (Cherenkov counters C_1, C_2 and C_3, scintillator counters S_1 and S_2) and detectors added for the test RUN. They include three more scintillator counters S_3, S_4 and S_μ, Cherenkov counter C_4, anticounter (Pb+Sci) with a hole A_0 and combined electromagnetic calorimeter EMC. Not shown in the figure are two blocks of proportional chambers PC1 and PC2 before M_7, which are not working and cannot be used as tracking detectors. The information about the detectors as well as some elements of the magnetic system is collected in Tab. 1.

4 Data taking

We generally used a simple trigger $T = S_1S_2S_3S_4\bar{A}_0$. For special runs we also used muon trigger $T_\mu = S_1S_2S_3S_4\bar{A}_0S_\mu$ as well as a loose trigger $T_L = S_1S_2S_3$.

The signals from the Cherenkov counters, EMC (3PM NaI and 1 PM LG), S_4 and for some runs from $\bar{A}_0$ were used in the amplitude analysis. This information can be used offline.

A time of flight system(TOF) was implemented (time difference between S_1 and S_4, C_1 and C_4, S_1 and C_4, etc). The behaviour of this system is currently not fully understood and it will be not used in the current analysis.

As it can be seen from Fig. 3 there were no working tracking detectors in December 2001 RUN. Thus we could not measure the momentum of the beam directly. Instead to have the beam with a certain momentum we used the known properties of the channel to adjust the currents of the magnetic elements. We guess that the real value of the momentum can differ from the nominal one by no more than 10-15%.

One major change in the geometry was introduced during the data taking. The Cherenkov counter C_4 was removed from the setup. The reason for this will be clear from the later text. Thus four main configurations (channel+detector) were used

- Scheme 1 with C_4 = Scheme 1a
- Scheme 2 with C_4 = Scheme 2a
- Scheme 1 without C_4 = Scheme 1b
- Scheme 2 without C_4 = Scheme 2b

Our usage of the channel was limited to five days in the beginning and five days at the end of the general IHEP RUN. In the first half of our time EMC was not intalled, so the data from this period of time can be used only for a rough estimate of the content of the beam.

Moreover, most of the time we were working in a 'parasitic' mode and could use only small fraction of proton beam. Thus our efforts were concentrated at the study of the efficiency of the electron tag rather than the absolute intensity of the electron beam.

Most of the data corresponds to 1 GeV secondary beam. Some data for higher energies is also available.

5 Analysis and results

General remarks

The main aim of the test RUN was to understand if we can develop the set of hardware (trigger) and software (amplitude analysis of Cherenkov and scintillator counters, guard counters, tracking detectors, etc) cuts in such a way that with a desired probability each software tag corresponds to the electron of the appropriate energy passing the tagging detectors and hitting the surface of the detector under study. To do this, we should have a calibrated detector with the inefficiency to the electrons at the desired level (say $\bar{\varepsilon} \leq 1 - 2 \cdot 10^{-5}$). Our current electromagnetic calorimeter seems to be adequate for this. It is homogeneous fully active detector almost without dead material. It has enough thickness ($\approx 19.5\ X_0$) and relatively good energy resolution (7-9% at 1 GeV). Thus, theoretically, for an electron with the momentum ≥ 1 GeV hitting the center of the detector, the energy ≤ 0.5 GeV should occur with the probability of $< 1 \cdot 10^{-5}$. In what follows we will consider the energy in the range 0.0-0.5 GeV as background region and relative number of the events in this region as the estimate of the inefficiency of the software electron tag.

Selection of electrons with Cherenkov counters

The correlation between the total energy in EMC and amplitude in C_1 is shown in Fig. 4. A typical cut for the electrons selection developed from this distribution reads $C_1 \geq 40$ counts. A similar cuts were developed for all other Cherenkov counters. Note that Fig. 4 corresponds to already calibrated EMC as described in the next subsection.

Calibration of the calorimeter

NaI light was collected with 3 PMT's (the 4th PMT was effectively dead), LG light was collected with 1 PMT. First signals from each NaI PMT were normalized w.r.t. LG. To do this, for the electrons identified with Cherenkov detectors we plotted distribution

$$E \sim N_{\mathrm{LG}} + N^{i}_{\mathrm{NaI}}\, C_i \tag{1}$$

where N are ADC counts after pedestal subtraction and C_i is calibration factor for i-th PMT. This distribution was fitted with a Gaussian and $\sigma(E)/E$ determined. Factor C_i was chosen at the minimum of $\sigma(E)/E$. After all C_i were found, expression

$$E \sim N_{\mathrm{LG}} + \frac{1}{3} \sum N^{i}_{\mathrm{NaI}}\, C_i \tag{2}$$

was normalized to the nominal beam energy of 1 GeV. Energy resolution of the combined calorimeter system at this energy was always a bit better than 10%.

The efficiency of the calorimeter

The inefficiency of the EMC for MIPs was measured using muon trigger. All the collimators were closed and intensity was rather low. About 5000 events were recorded. The results can be seen in Fig. 5. We find only one suspicious event with the total energy in EMC ≈ 90 MeV, the most probable value for MIP being 300 MeV. We can conclude that the inefficiency of EMC for muons is not worse than $2 \cdot 10^{-4}$.

To estimate the level of the inefficiency of the EMC, which can be achieved with the current configuration, we developed simple GEANT-based Monte-Carlo program. It was supposed that the electrons in the beam were tagged by the Cherenkov counters. The electrons were simulated as a pencil beam originated in the middle of the M_7-magnet and passing through the centers of the S_3 and S_4 counters. The response of the EMC was simulated in a oversimplified way as being proportional to the dE/dx. All the material between the origin of the electrons and the end of EMC was taken into account. 100000 events were generated. The results after the simulation of the trigger ($S_3 S_4 \bar{A}_0$) are shown in Fig. 6 for 1 GeV beam. We found about 5 suspicious events with the total energy in EMC ≤ 0.5 GeV. Although our beam has nonzero space and angular spread, we can definitely conclude that with the current EMC we are able to tag the electron with the inefficiency of the order of $1 \cdot 10^{-4}$.

Achieved inefficiency levels

We start presenting the results of the test RUN with the data of Scheme 1a configuration for 1 GeV beam. As it can be seen from Fig. 7, the inefficiency of electron tagging by the trigger and software cuts are not so good - at the level of 1-3%. Here and for all similar pictures the cut number means

- first point: no cuts
- second point: C_1 cut
- third point: + C_2 cut
- forth point: + C_3 cut
- fifth point: + C_4 cut (if any)

The situation for 3 GeV beam in the same configuration seems to be a little bit better - see Fig. 8.

The change of the configuration (Scheme 1 $\rightarrow$ Scheme 2) does not help a lot - see Fig. 9. Although the fraction of electrons in the beam for this configuration is much greater than for Scheme 1, the final result is basically the same.

The situation has changed significantly after removal of the C_4 from the channel (Fig. 10). It turned out that C_4-cut kills the background created by C_4 itself, but only partly!

More detailed comparison between Scheme 2a and 2b can be seen on Figs. 11 and 12. The background for Scheme 2b configuration has rather peculiar features - all background events have very small energy in EMC, although the amplitude of the signal in S_4 seems to be normal MIP. The origin of this background is still unclear - we do not have enough statistics to study it. If we assume that its origin lies in some electronics failures or in some kind of a random coincidence and ignore it for a moment - than the level of the tagging inefficiency achieved for this configuration would be $\leq 2.5 \cdot 10^{-4}$, which is close to the MC value.

The last picture we would like to present is the background level for Scheme 1b (Fig. 13). The background for this configuration is better than for Scheme 1a, but worse than for Scheme 2b by a factor of 5-7 (if we again ignore low energy events in EMC). If we don't ignore them, than 2b is better than 1b by a factor of 2.

The results of the RUN are summed in Tab. 2.

6 Future plans

We think that obtained results justify further efforts at the 18T channel. We see followings ways to reduce background level and/or to give us better understanding of what is going on.

- Minimize material in the beam.
  This includes removal of unused detectors off the beam line, usage of He bags, lowering pressure in Cherenkov detectors.

- Improve veto system.
  This should reduce level of accidental activity and guard against interactions of the beam e^+.

- Measure momentum of beam particles event by event.
  To do this we plan to construct system of three scintillation hodoscopes.

- Increase event rate.
  It is straightforward to move calorimeter closer to the last magnet. Also we will try to understand safety limitations on the proton flux on the primary target.

- More detailed and accurate Monte-Carlo simulation, including the elements of the magnetic system of the channel.

We will consider possibility to create electron beam on the channel of the ISTRA facility.

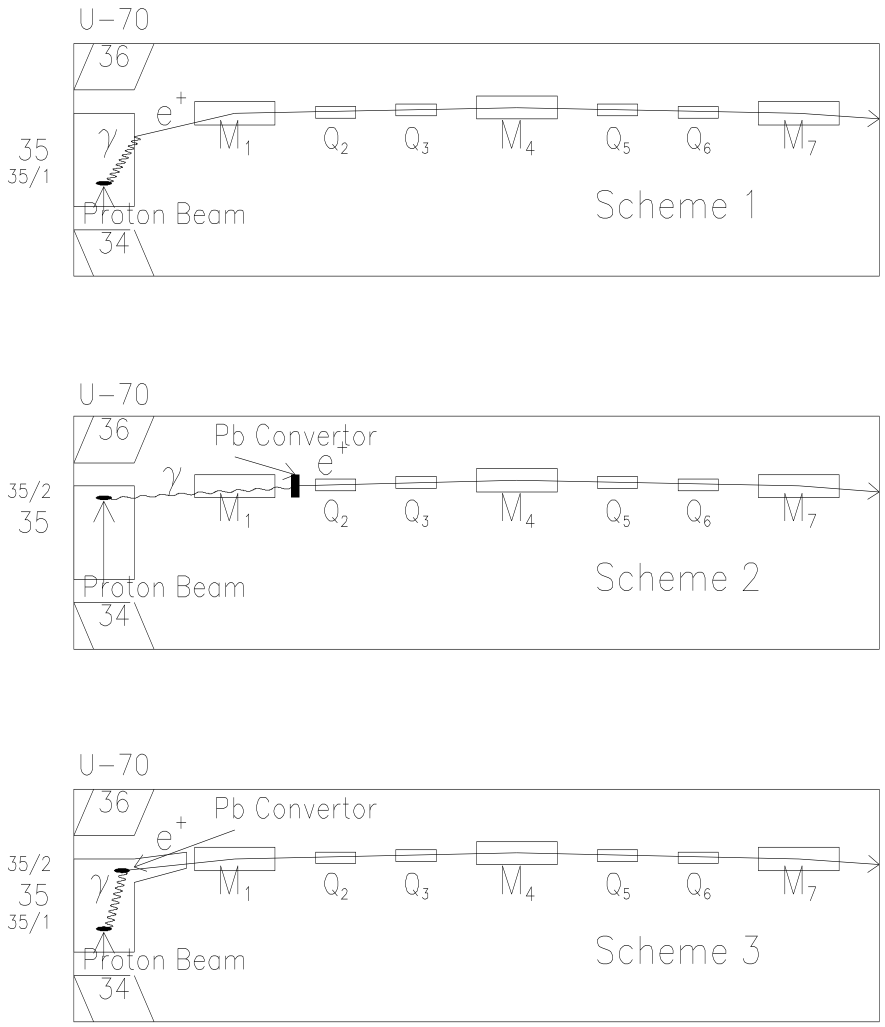

Figure 1: Possible schemes for electron beam at CH18T. Schemes 1 and 2 were used during December 2001 RUN. Scheme 3 requires modification of the vacuum chamber and target stand of the 35 block.
M-dipole magnets, Q-quadrupole magnets, 34,35,36 - blocks of U-70, 35/1 and 35/2 - internal targets. The figures are not to the scale

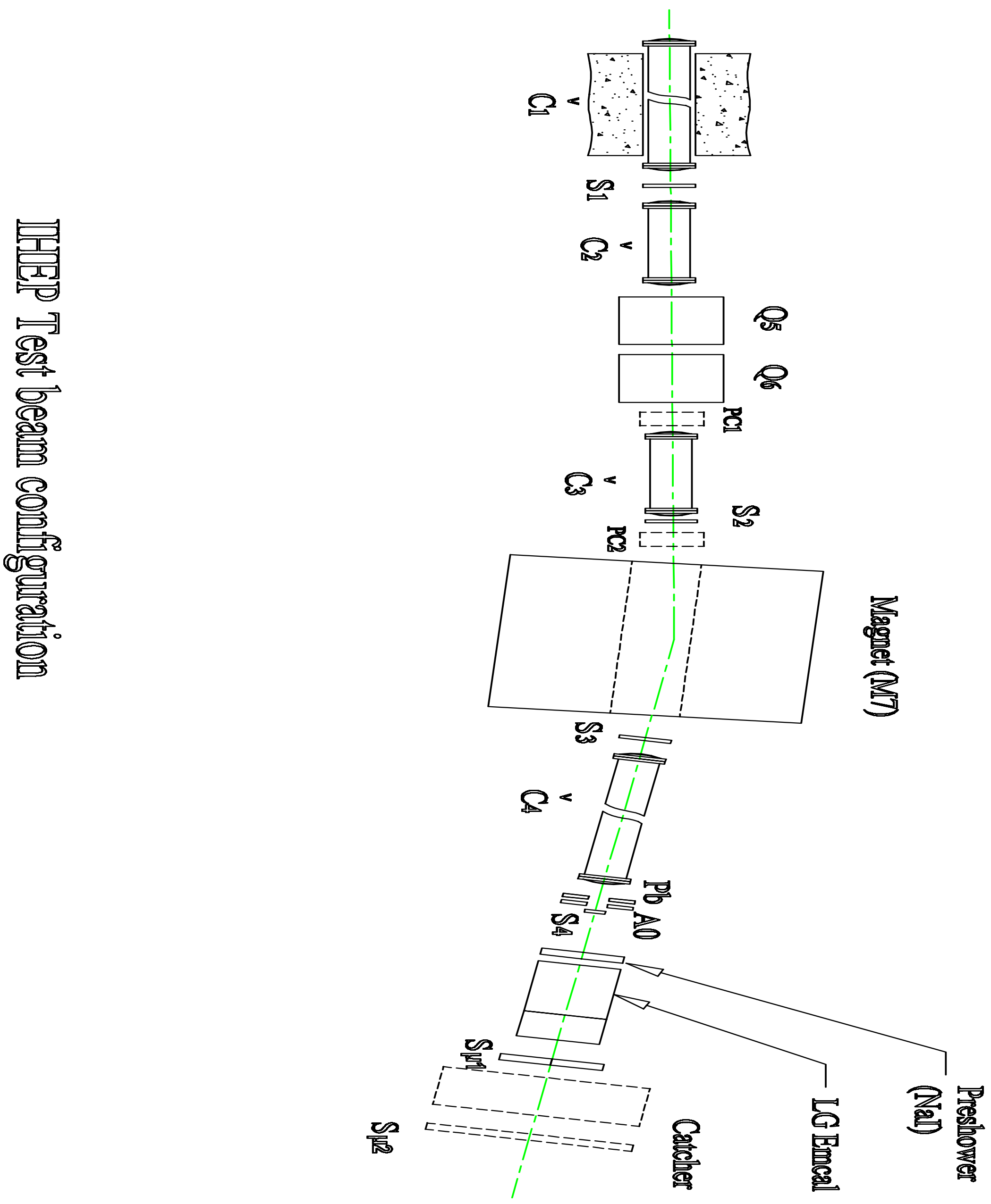

Figure 2: View of the setup used in the December 2001 RUN.

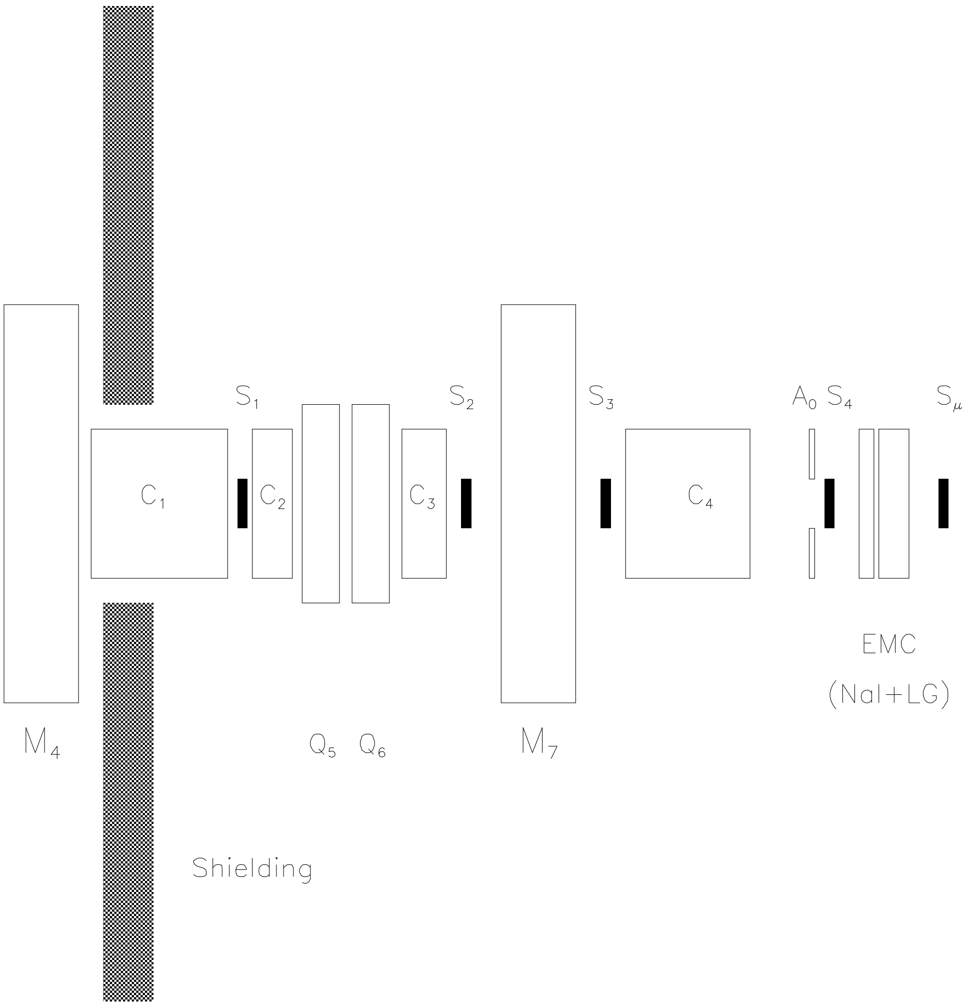

Figure 3: Schematic view of the setup used in the December 2001 RUN. M-dipole magnets, Q-quadrupole magnets, C-Cherenkov counters, S-scintillator counters, A-guard counter, EMC-combined electromagnetic calorimeter. The figure is not to the scale.

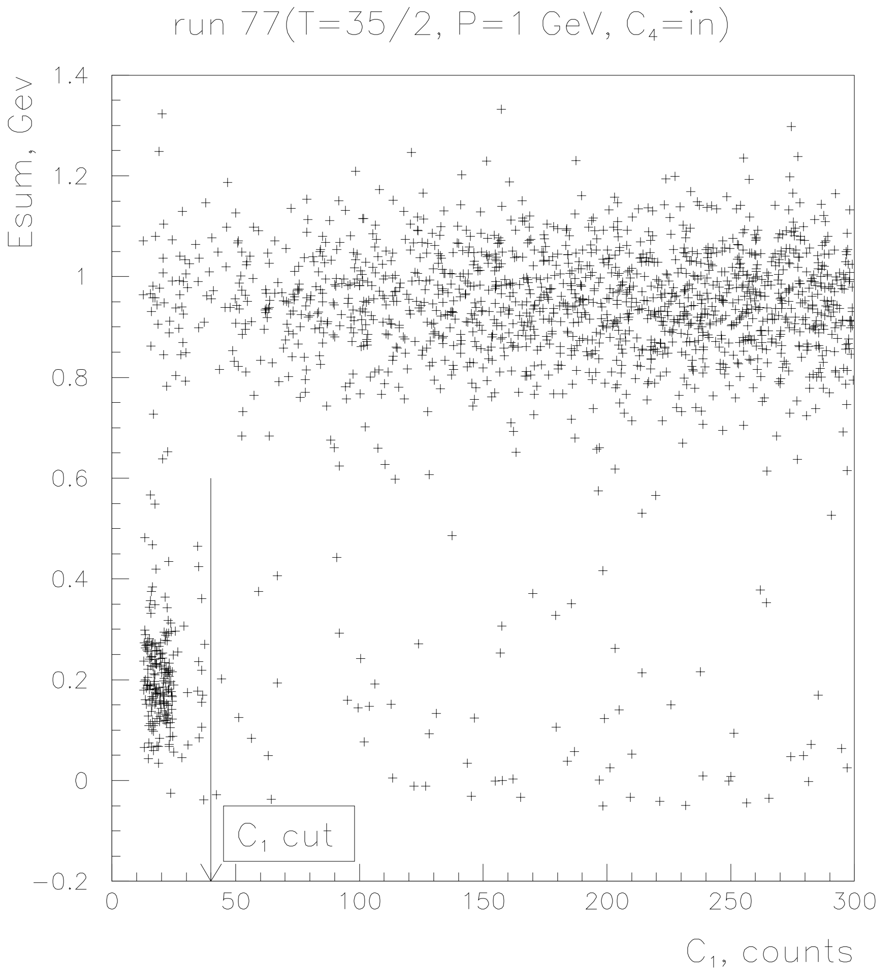

Figure 4: The correlation between the total energy in EMC and amplitude in C_1

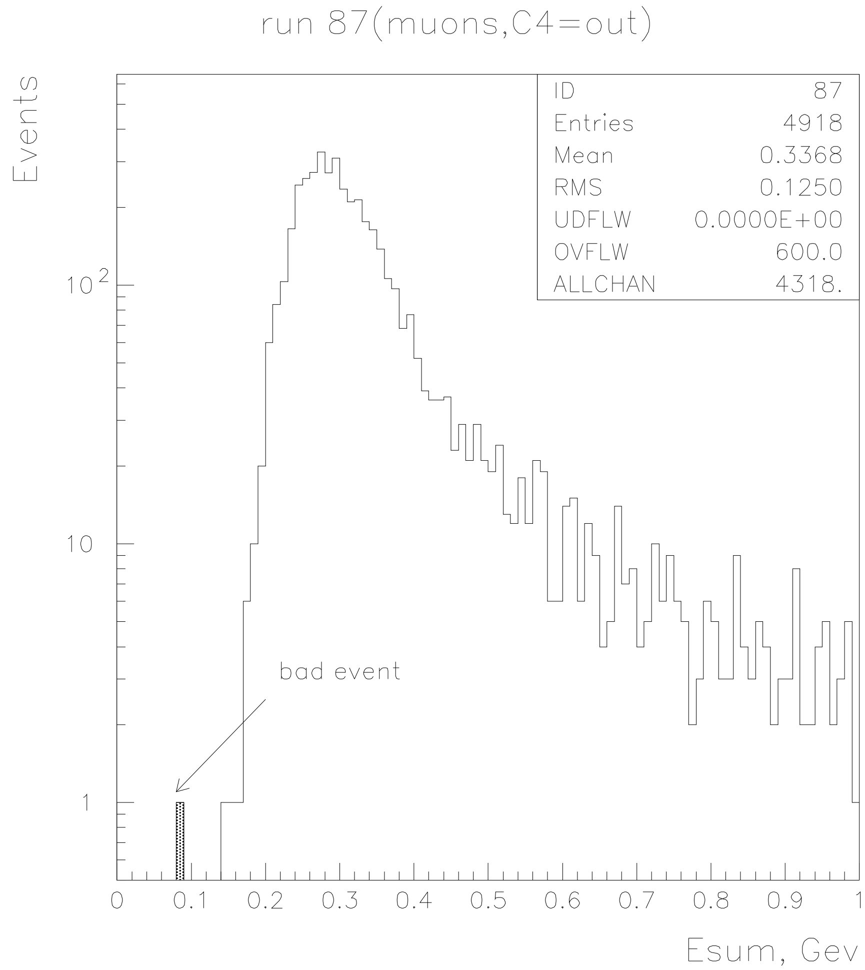

Figure 5: Total energy in EMC for 'muon' events

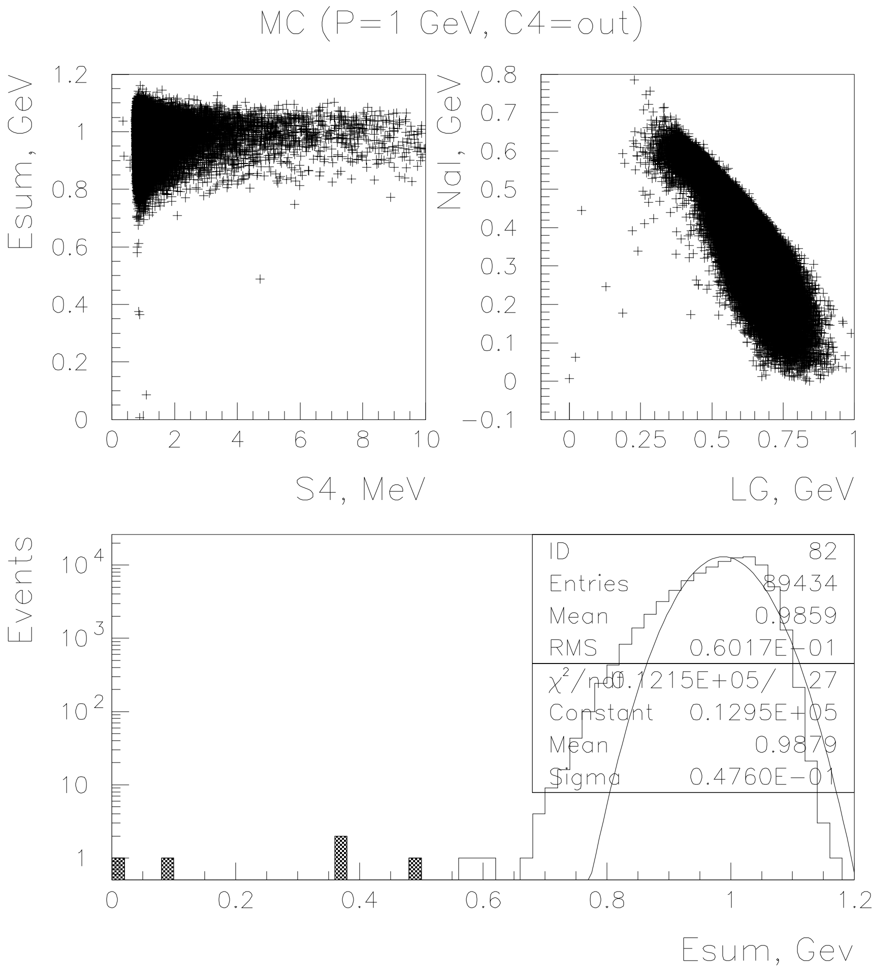

Figure 6: MC run 1 Gev. Left upper picture - total energy in EMC vs the energy in S_4; right upper picture - energy in NaI vs energy in PG; lower picture - the distribution of the total energy in EMC. The integrals of the dE/dx in NaI and LG were weighted and summed with 1 GeV normalization.

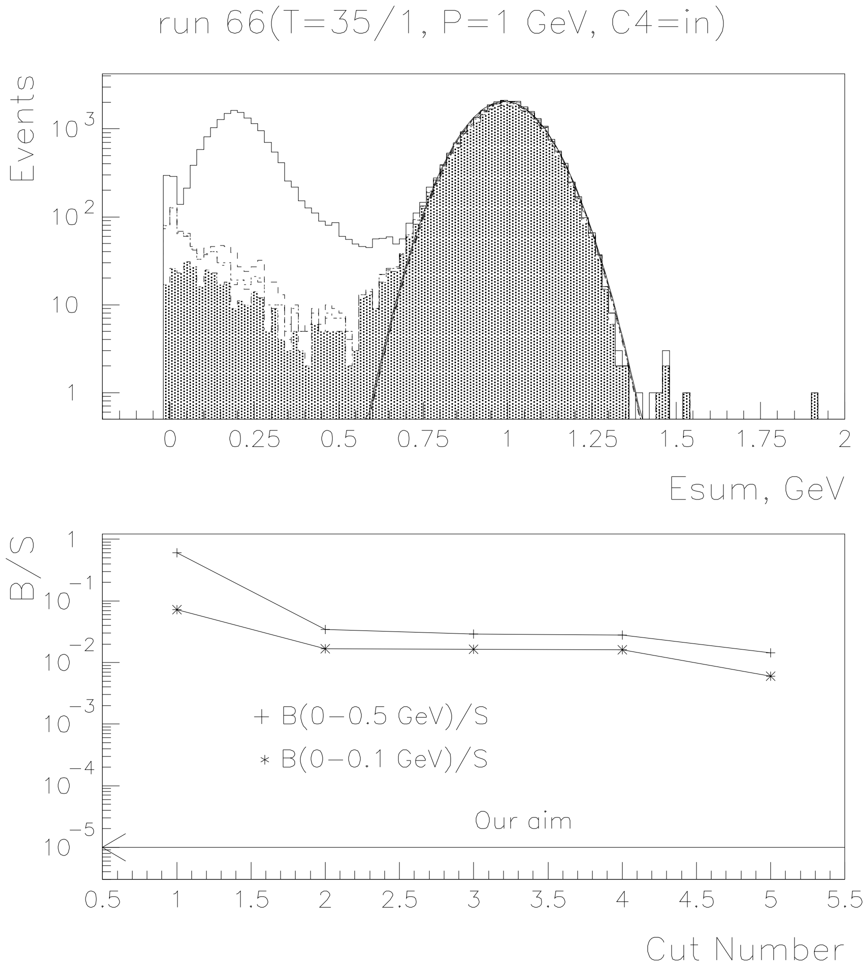

Figure 7: run 66 = Scheme 1a. Upper picture - the distribution of the total energy in EMC for the sequence of cuts; lower picture - the ratio of the number of background events to the total number of events after cut vs cut number.

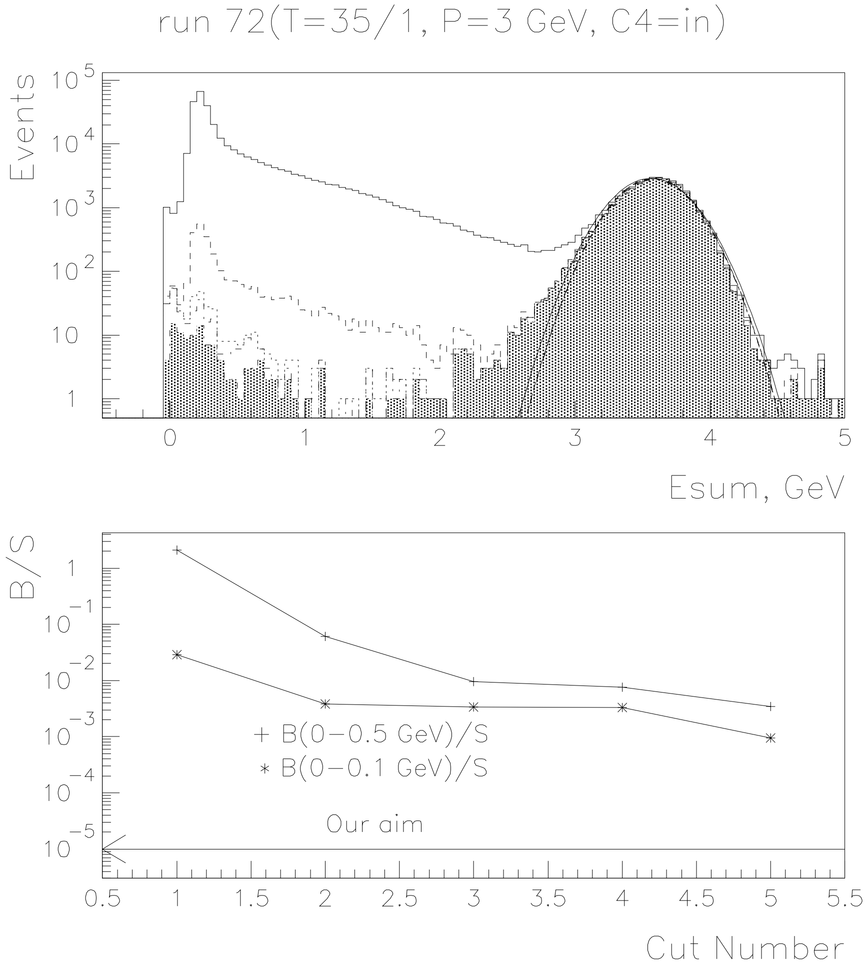

Figure 8: run 72 = Scheme 1a. Upper picture - the distribution of the total energy in EMC for the sequence of cuts; lower picture - the ratio of the number of background events to the total number of events after cut vs cut number.
[run 72]

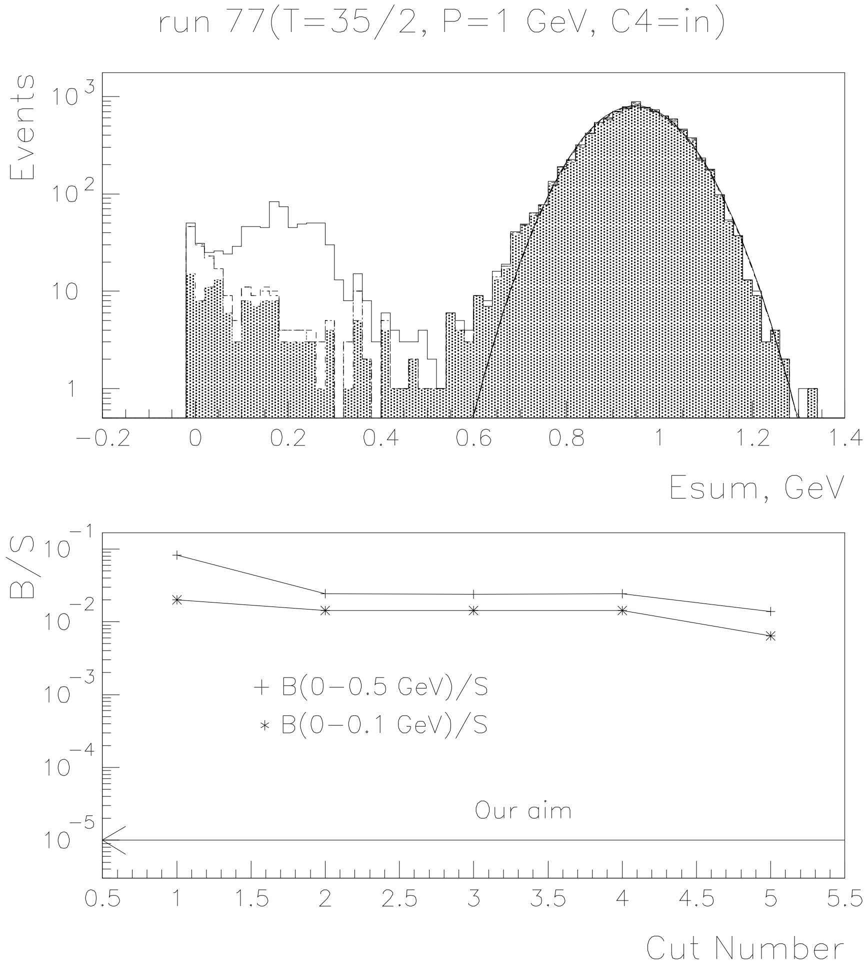

Figure 9: run 77 = Scheme 2a. Upper picture - the distribution of the total energy in EMC for the sequence of cuts; lower picture - the ratio of the number of background events to the total number of events after cut vs cut number.
[run77]

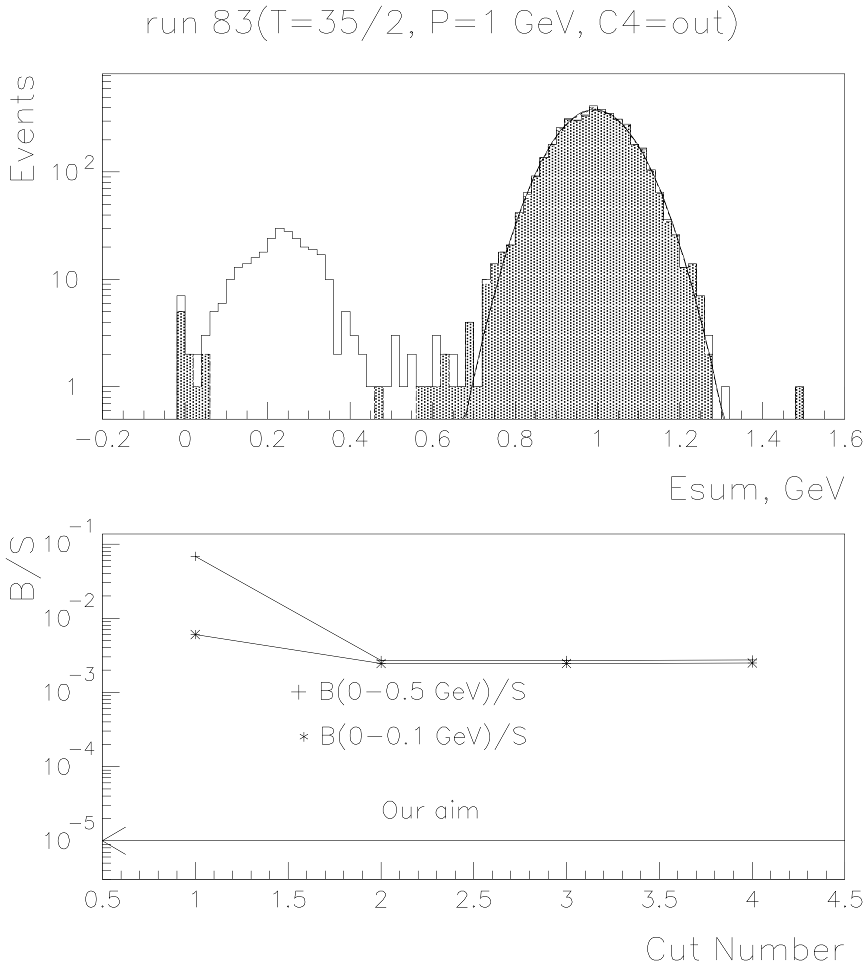

Figure 10: run 83 = Scheme 2b. Upper picture - the distribution of the total energy in EMC for the sequence of cuts; lower picture - the ratio of the number of background events to the total number of events after cut vs cut number.

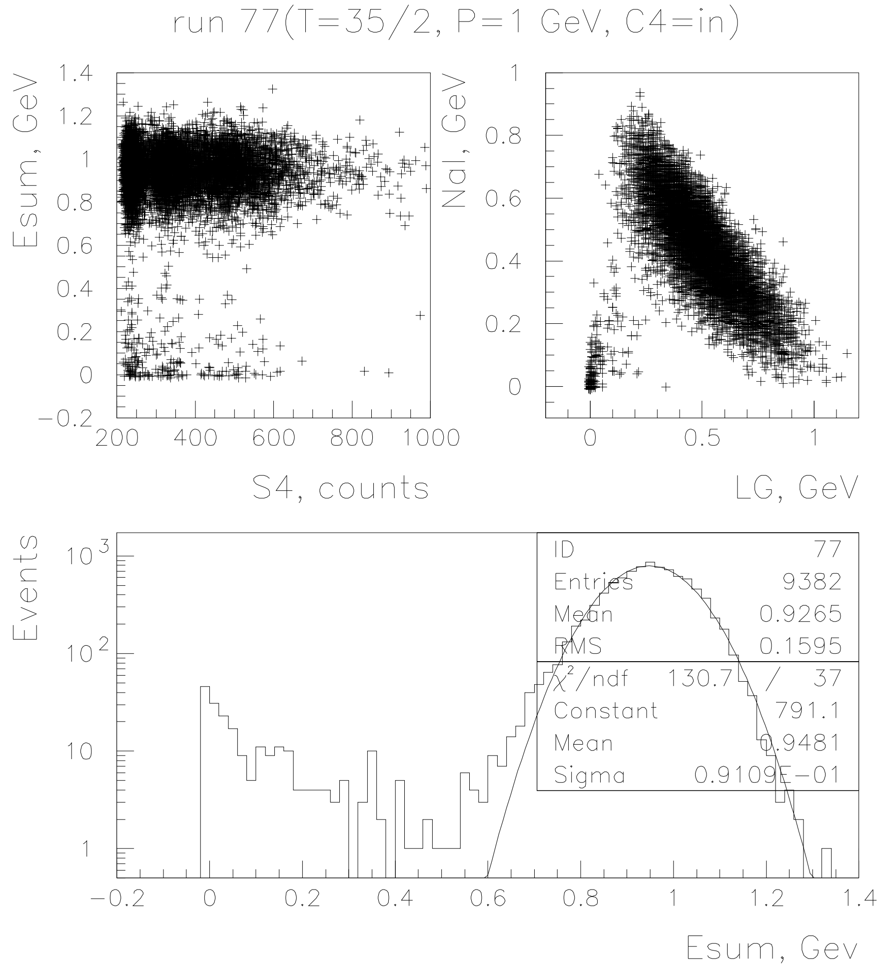

Figure 11: run 77 = Scheme 2a. Left upper picture - total energy in EMC vs the amplitude in S_4; right upper picture - energy in NaI vs energy in PG; lower picture - the distribution of the total energy in EMC.

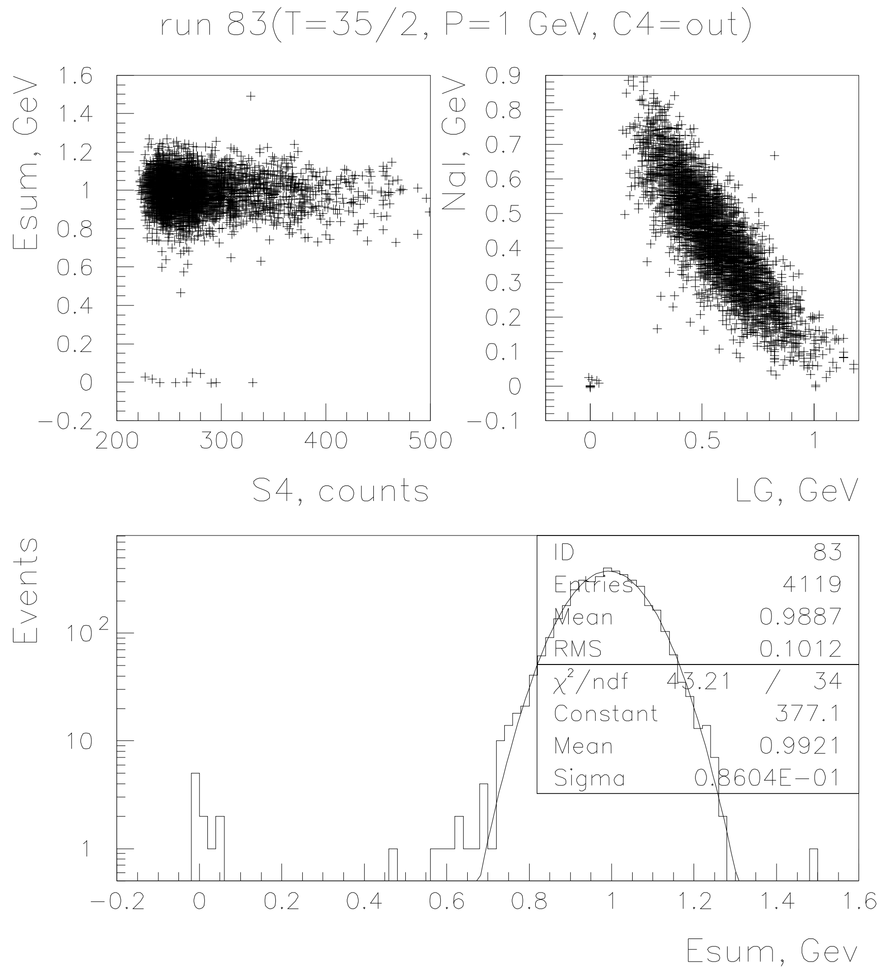

Figure 12: run 83 = Scheme 2b. Left upper picture - total energy in EMC vs the amplitude in S_4; right upper picture - energy in NaI vs energy in PG; lower picture - the distribution of the total energy in EMC.

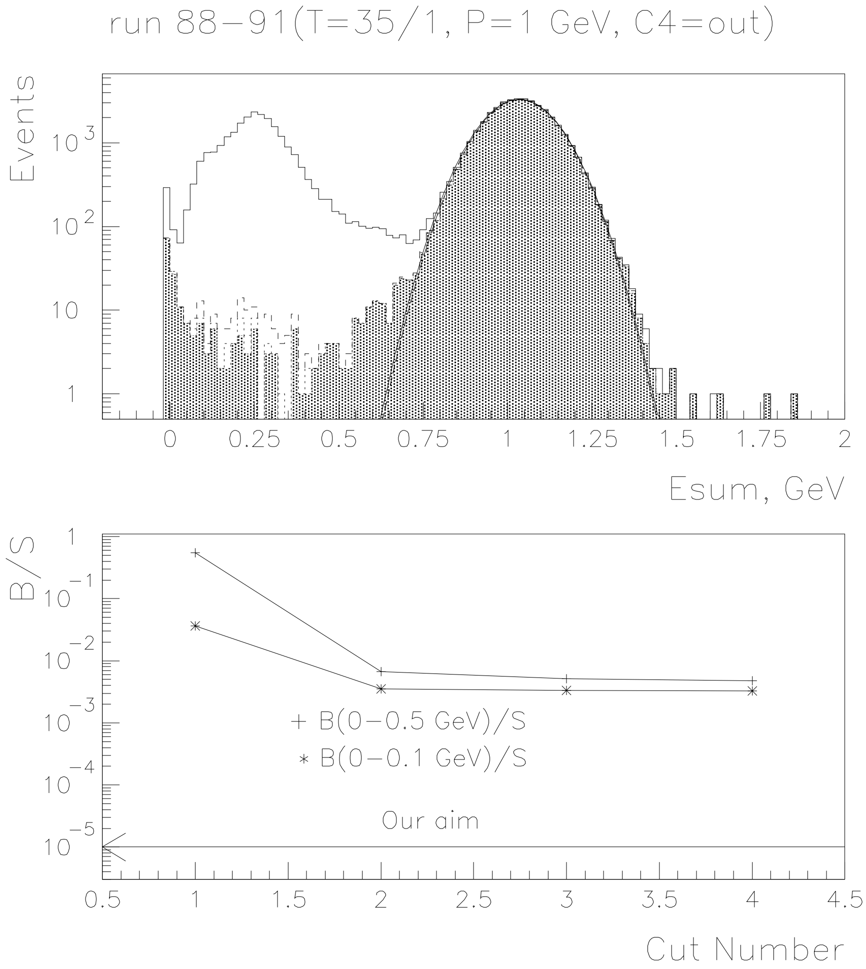

Figure 13: run 88-91 = Scheme 1b. Upper picture - the distribution of the total energy in EMC for the sequence of cuts; lower picture - the ratio of the number of background events to the total number of events after cut vs cut number.

Table 1: Positions and some characteristics of used apparatus and some elements of the magnetic system. The values of Z are relative to the center of C_1.

Name	Material	Z center cm	ΔZ, cm	ΔX x ΔY, cm^2	Additional information
C_1	Air (0.5 atm)	0	710.0	21(diam)	mylar flanges
S_1	PS	360	1.0	12(diam.)	
C_2	Air (0.5 atm)	437	130.0	21(diam)	1 mm Al flanges
Q_5	Air	610	100.0	20(diam)	
Q_6	Air	775	100.0	20(diam)	
$PC1$	$\approx$ 2 mm Al	870		20x20	
C_3	Air (0.5 atm)	1010	190.0	21(diam)	mylar flanges
S_2	PS	1115	0.5	12(diam.)	
$PC2$	$\approx$ 2 mm Al	1130		40x40	
M_7	Air	1405	400.0		
S_3	PVT(BC404)	1660	0.5	6.5x6.5	
C_4	Air (0.25 atm)	1960	600.0	21(diam)	mylar flanges
A		2284			Sandwich
	Pb		0.4	25x25	hole 5 cm
	PS		2.0	24x24	hole 5 cm, 2 PM
S_4	PVT(BC404)	2287	0.5	5.4x5.4	
NaI	Na(I)	2352	10.0	20(diam.)	3.9 X_0, 4 PM
LG	SF5	2377	40.0	20x20	11 mm Al+1 mm Fe + 15.4 X_0
S_μ	PS	2422	50.0	5x9	

Table 2: Background levels for different runs. Events-number of electrons in the sample, BGR-0 - B/S in the 0-0.5 GeV range, BGR-1 - B/S in the 0.1-0.5 GeV range

TGT	run	Events	BGR-0	BGR-1	Trigger (T)	Notes
35/1	66	26280	$3.4 \cdot 10^{-2}$	$1.6 \cdot 10^{-2}$	$S1\,S2\,S3\,S4\,\bar{A}$	1a (with $C4$)
35/2	77	9382	$2.3 \cdot 10^{-2}$	$1.4 \cdot 10^{-2}$	$S1\,S2\,S3\,S4\,\bar{A}$	2a (with $C4$)
35/2	83	4119	$2.6 \cdot 10^{-3}$	$2.4 \cdot 10^{-4}$	$S1\,S2\,S3\,S4\,\bar{A}$	2b (w/o $C4$)
35/1	88–91	40257	$4.7 \cdot 10^{-3}$	$1.8 \cdot 10^{-3}$	$S1\,S2\,S3\,S4\,\bar{A}$	1b (w/o $C4$)